Geochimica et Cosmochimica Acta Vol. 57, pp. 3001–3011

0016-7037/93/$6.00 + .00

Heat capacities of TiO_2-bearing silicate liquids: Evidence for anomalous changes in configurational entropy with temperature

REBECCA A. LANGE[1] and ALEXANDRA NAVROTSKY[2]

[1]Department of Geological Sciences, University of Michigan, Ann Arbor, MI 48109, USA
[2]Department of Geological and Geophysical Sciences, Princeton University, Princeton, NJ 08544, USA

(*Received July* 24, 1992; *accepted in revised form December* 29, 1992)

Abstract—The heat capacities of several TiO_2-bearing silicate glasses and liquids containing Cs_2O, Rb_2O, Na_2O, K_2O, CaO, MgO, or BaO have been measured to 1100 K using a differential scanning calorimeter and to 1800 K using a Setaram HT-1500 calorimeter in step-scanning mode. The results for liquids of M_2O-TiO_2-$2SiO_2$ composition (M = Na, K, Cs) are compared to those for liquids of M_2O-$3SiO_2$ composition. The presence of TiO_2 has a profound influence on the heat capacity of simple three-component silicate liquids over the temperature range 900–1300 K. Specifically, replacement of Si^{4+} by Ti^{4+} leads to doubling of the magnitude of the jump in C_p at the glass transion (T_g); this is followed by a progressive decrease in liquid C_p for over 400 K, until C_p eventually becomes constant and similar to that in Ti-free systems. The large heat capacity step at T_g in the TiO_2-bearing melts suggests significant configurational rearrangements in the liquid that are not available to TiO_2-free silicates. In addition, these "extra" configurational changes apparently saturate as temperature increases, implying the completion of whatever process is responsible for them, or the attainment of a random distribution of structural states. Above 1400 K, however, where the heat capacities of TiO_2-bearing and TiO_2-free alkali silicate liquids are similar, their configurational entropies differ by ~3.5 J/g.f.w.-K. The larger configurational entropy of the TiO_2-bearing alkali silicate liquids relative to the TiO_2-free liquids is energetically equivalent to raising the liquid temperature by more than 300 degrees. This result clearly demonstrates the energetic magnitude of the configurational changes apparent in the supercooled liquid region and their impact on the thermodynamic properties of the stable liquid. Consideration of both density measurements on liquids and spectroscopic data on quenched glasses (from the literature) suggests that the anomalous configurational rearrangements may involve the breakdown of alkali and alkaline earth titanate complexes and changes in Ti^{4+} coordination.

INTRODUCTION

CURRENTLY, THERE ARE only four TiO_2-bearing silicate liquids for which heat capacity measurements have been reported: $CaTiSiO_5$ (KING et al., 1954), $Na_2TiSi_2O_7$, $K_2TiSi_2O_7$ (RICHET and BOTTINGA, 1985), and a liquid in the Na_2O-TiO_2-SiO_2 system whose composition does not correspond to a crystalline compound (CARMICHAEL et al., 1977). This is a sparse data set, especially considering that TiO_2 can be a major component in magmatic liquids, ranging up to 10 wt% in alkali-rich, silica-poor lavas such as ugandites and lamproites (e.g., WATERS, 1987). In addition, the measured heat capacities of the alkali-titania-silicate melts display a complex negative temperature dependence (RICHET and BOTTINGA, 1985) that makes it difficult to use the current data set to accurately predict the effect of TiO_2 on the heat capacities of natural melt compositions. The data in the present study confirm that the presence of TiO_2 has a profound influence on the heat capacity of simple three-component silicate liquids over the temperature range at which magmas crystallize (900–1350 K). Perhaps most importantly, the unusual behavior of the heat capacity with temperature observed for $Na_2TiSi_2O_7$ and $K_2TiSi_2O_7$ melts may provide key information on the configurational changes available to alkali silicate liquids containing Ti^{4+} and requires more detailed examination.

In this study, we demonstrate that there is a significant change in the configurational heat capacity when one mole of TiO_2 replaces one mole of SiO_2 in R_2O-$3SiO_2$ and R_2O-$2SiO_2$ liquids (R = Na, K, Rb, Cs). We also present C_p measurements on TiO_2-bearing silicate liquids containing BaO, CaO, and MgO. These data are discussed in the context of available density, viscosity, and spectroscopic measurements. In addition to their own intrinsic interest, the titanium-bearing melts may be useful analogues for studying the effects of coordination change on the thermodynamic and transport properties of silicate melts at lower mantle pressures.

EXPERIMENTAL METHODS

The compositions investigated were prepared by mixing appropriate proportions of reagent grade oxides and carbonates. Samples were fused, quenched to a glass, ground to a powder, and re-fused at 1373 K. This procedure was repeated twice (for a total of four fusions) to ensure homogeneity. The glass samples were analyzed (Table 1) using the JEOL 8600 electron microprobe at Rutgers University and the Cameca CAMEBAX electron microprobe at the University of Michigan. Standard operating conditions consisted of a focused electron beam in raster mode, an accelerating potential of 15 kV, and a sample current of 10 nA. Standards included Na_2O-TiO_2-SiO_2, K_2O-TiO_2-SiO_2, and CaO-MgO-TiO_2-SiO_2 glasses analyzed by wet chemical methods.

Those samples for which heat capacity measurements were made in the supercooled liquid region (all alkali-bearing samples) were examined both optically and by X-ray diffraction (XRD) for any incipient crystallization. All samples appeared clear and transparent. However, the XRD pattern for the K_2O-TiO_2-SiO_2 sample revealed a broad peak suggestive of cryptocrystalline K_2TiSiO_5; all other samples showed no evidence for crystallization.

Table 1a. Electron microprobe analyses of glass samples (wt %).

	CMTS	BTS_2	NTS_2	KTS_2	KTS	$RbTS_2$	$CsTS_2$	CsS_3
SiO_2	37.85	33.63	46.31	40.33	28.14	34.42	26.51	36.25
TiO_2	19.27	23.92	33.11	29.27	34.78	23.02	17.48	---
MgO	12.30	---	---	---	---	---	---	---
CaO	29.50	---	---	---	---	---	---	---
BaO	---	42.39	---	---	---	---	---	---
Na_2O	---	---	20.41	---	---	---	---	---
K_2O	---	---	---	29.22	36.66	---	---	---
Rb_2O	---	---	---	---	---	42.56*	---	---
Cs_2O	---	---	---	---	---	---	54.54	63.11
Total	98.92	99.94	99.83	98.82	99.58	100.00*	98.53	99.36

Calorimetric measurements over the temperature interval 473–1090 K were made with a Setaram DSC-111 differential scanning calorimeter under flowing air. Powdered samples (125–143 mg) were packed into a cylinderical Pt crucible and covered with a Pt lid. Measurements were made over four temperature intervals: 473–678 K, 643–818 K, 783–968 K, and 923–1090 K. A single run over a specific temperature interval (taking approximately 3 h) involved a series of steps in which the sample was heated at a rate of 2 K/min for 5 min, followed by isothermal equilibration for 5 min. The following sequence of experiments were performed over each temperature interval: two blank runs (empty crucible + lid), two calibration runs (powdered corundum), three sample runs, two blank runs, and two calibration runs. The average of the blank runs was subtracted from the average of the calibration and sample runs to correct for baseline effects, and the C_p data of ROBIE et al. (1978) for corundum were used to derive C_p values for the samples. The accuracy of this procedure was evaluated by measuring the C_p of silica glass; our results are within 2% of those of RICHET et al. (1984). We estimate our precision in C_p (based on the reproducibility of individual runs) to be ±3–4%.

High temperature (750–1800 K) C_p measurements were made in air with a Setaram HT-1500 calorimeter in step-scanning mode. In this approach, the change in enthalpy of a sample was measured during heating (or cooling) over a small temperature interval (10 K), thus providing a measurement of heat capacity. The apparatus and experimental procedure have been described in detail by LANGE et al. (1991) and LANGE and NAVROTSKY (1992). In brief, the calorimetric detector consists of an upper and lower thermopile surrounding a sample and reference chamber respectively. Approximately 1 g of sample was held in a Pt crucible that was contained within the sample chamber. During a step-scanning run, the thermopile voltage was monitored as the temperature was raised (or lowered) at a rate of 1 K/min over 10 K. A 10 min heating (or cooling period) was followed by a 15 min isothermal period to allow thermal equilibration (and the voltage to return to baseline). A typical run consisted of ten alternating heating and cooling steps (up and down over the same 10 K interval). The average of the integrated areas under ten voltage peaks represents one datum point. A single, step-scanning experiment consisted of three runs: a blank (empty Pt crucible), a calibration (corundum powder), and a sample. As for the DSC-111 procedures, the results of the blank were subtracted from those of the calibration and sample runs, and the C_p data of ROBIE et al. (1978) were used to derive C_p values for the samples. A detailed discussion of the precision and accuracy of these experiments is found in LANGE and NAVROTSKY (1992). The standard deviations on the average integrated areas for the blank, calibration, and sample runs lead to a propagated error on C_p (sample) that varies from 5–10%. However, for those samples that display no temperature dependence to their liquid C_p (the BaO- and CaO-MgO-bearing samples), fitted standard deviations on C_p (sample) range from 2–3%. The difference between individual and fitted error estimates has been discussed by LANGE and NAVROTSKY (1992).

Table 1b. Electron microprobe analyses of glass samples (mol %)†.

	CMTS	BTS_2	NTS_2	KTS_2	KTS	$RbTS_2$	CsTS2	CsS_3
SiO_2	37.00	49.29	50.89	49.80	36.23	52.62	51.69	72.93
TiO_2	14.17	26.36	27.36	27.18	33.67	26.47	25.63	---
MgO	17.93	---	---	---	---	---	---	---
CaO	30.90	---	---	---	---	---	---	---
BaO	---	24.35	---	---	---	---	---	---
Na_2O	---	---	21.74	---	---	---	---	---
K_2O	---	---	---	23.02	30.10	---	---	---
Rb_2O	---	---	---	---	---	20.91*	---	---
Cs_2O	---	---	---	---	---	---	22.67	27.07

*Rb_2O determined by difference.
†Note that the analyzed compositions deviate from the nominal compositions (e.g., 50 mole % SiO_2, 25 mole % TiO_2, 25 mole %Na_2O is the nominal composition for NTS2).

RESULTS

Heat capacity measurements are reported in Table 2 and Figs. 1–5. Fitted three-term Maier-Kelley equations to the glass C_p data are also presented. The primary motivation for the DSC measurements on the glasses was to directly observe the heat capacity across the glass transition. The importance of this is demonstrated in Fig. 1 where the variation in heat capacity with temperature for Na_2O-$3SiO_2$ glass and liquid (RICHET et al., 1984) is compared to that measured in this study for Na_2O-TiO_2-$2SiO_2$ glass and liquid. The striking feature of this diagram is that replacement of Ti^{4+} for Si^{4+} leads to doubling of the magnitude of the jump in C_p at the glass transition. Moreover, the C_p of Na_2O-TiO_2-$2SiO_2$ liquid decreases with increasing temperature over an interval of ~400 K until it eventually becomes constant and similar to that seen for Na_2O-$3SiO_2$ over the entire liquid range. This negative temperature dependence of the Na_2O-TiO_2-$2SiO_2$ liquid C_p was also observed by RICHET and BOTTINGA (1985); their fitted curve is shown in Fig. 1b for comparison.

It is important to point out that our DSC measurements of C_p (solid circles in Fig. 1b) were not obtained under rapid scanning conditions (e.g., 20 K/min is a common scan rate for published DSC C_p data). Instead, measurements were made under relatively slow step-scanning conditions (2 K/min for 5 min followed by 5 min of isothermal equilibration). As a consequence, the jump in C_p at T_g and the subsequent negative temperature dependence to the liquid C_p obtained from the DSC measurements are not caused by "overshooting" the transition because of rapid scanning rates. Moreover, the step-scanning run through the glass transition was repeated three times and was reproducible within error.

To evaluate the possible effect of incipient crystallization in the supercooled liquid on the heat capacity vs. temperature curve, the Na_2O-TiO_2-$2SiO_2$ sample was held at 923 K for 30 h prior to a DSC run between 923–1090 K. The results from this experiment are shown in Fig. 2 by the open circles; the data indicate that crystallization of the supercooled liquid

Table 2a. Fit equations to heat capacities of individual glasses; $Cp = a + bT + cT^{-2}$ gfw.

Sample	a	$b \times 10^2$	$c \times 10^{-5}$	σ	T_g (K)
NTS2	57.20	2.678	-10.63	1.7	810
KTS2	68.43	1.200	-20.11	0.6	790
RbTS2	66.43	0.8117	-15.09	1.9	787
CsTS2	56.56	2.068	-14.25	1.9	785
CsS3	70.57	-0.2212	-28.24	0.2	777

gfw = gram formula weight
σ = standard error of the estimate
T_g = glass transition temperature

Table 2b. Supercooled and stable liquid heat capacity measurements (J/g.f.w.-K) for each composition.

Sample	T(K)	Cp^{meas}	Sample	T(K)	Cp^{meas}
NTS2	831.18	83.52	KTS2	920.79	108.88
NTS2	841.14	100.30	KTS2	930.69	105.14
NTS2	851.15	103.89	KTS2	930.79	108.18
NTS2	861.13	108.96	KTS2	940.61	104.99
NTS2	871.07	111.42	KTS2	940.79	105.99
NTS2	881.03	110.98	KTS2	950.57	103.18
NTS2	890.92	109.97	KTS2	950.77	104.98
NTS2	900.91	107.51	KTS2	960.74	101.46
NTS2	910.84	105.40	KTS2	970.70	103.93
NTS2	920.79	111.18	KTS2	980.59	105.69
NTS2	930.69	109.42	KTS2	990.48	102.69
NTS2	940.61	109.11	KTS2	1000.39	102.37
NTS2	941.70	108.39†	KTS2	1010.32	103.47
NTS2	950.57	105.32	KTS2	1020.25	101.20
NTS2	1006.90	108.74†	KTS2	1030.20	98.73
NTS2	1119.40	105.06†	KTS2	1040.17	97.12
NTS2	1271.90	98.31†	KTS2	1050.15	104.75
NTS2	1341.70	95.12†	KTS2	1060.02	97.55
NTS2	1414.60	93.76†	KTS2	1069.89	96.80
NTS2	1533.20	93.93†	KTS2	976.10	104.53†
NTS2	1651.50	93.44†	KTS2	1077.40	98.83†
NTS2	1761.20	90.76†	KTS2	1151.90	102.33†
KTS2	791.47	74.57	KTS2	1201.20	96.05†
KTS2	791.94	76.88	KTS2	1268.50	94.02†
KTS2	801.41	77.08	KTS2	1321.20	91.38†
KTS2	801.84	76.65	KTS2	1444.70	86.21†
KTS2	811.34	79.45	KTS2	1516.10	91.34†
KTS2	821.22	86.77	KTS2	1615.40	92.13†
KTS2	831.18	102.08	KTS2	1731.30	89.06†
KTS2	841.14	104.14	RbTS	791.47	75.17
KTS2	851.15	108.10	RbTS	801.41	80.90
KTS2	861.13	106.75	RbTS	811.34	85.92
KTS2	871.07	105.78	RbTS	821.22	94.80
KTS2	881.03	107.65	RbTS	831.18	94.26
KTS2	890.92	107.60	RbTS	841.14	99.57
KTS2	900.91	105.09	RbTS	851.15	95.60
KTS2	910.84	108.29	RbTS	861.13	96.73
KTS2	920.73	107.21	RbTS	871.07	102.02
RbTS	881.03	98.70	CsTS	910.84	99.47
RbTS	890.92	102.90	CsTS	920.73	102.72
RbTS	900.91	97.68	CsTS	920.79	102.73
RbTS	910.84	97.65	CsTS	930.69	100.04
RbTS	920.73	101.70	CsTS	930.79	101.12
RbTS	920.79	102.18	CsTS	940.61	99.40
RbTS	930.69	95.88	CsTS	940.79	99.28
RbTS	930.79	95.48	CsTS	950.57	97.10
RbTS	940.61	101.56	CsTS	950.77	91.75
RbTS	940.79	100.93	CsTS	960.74	91.86
RbTS	950.57	96.54	CsTS	970.70	92.28
RbTS	950.77	95.98	CsTS	980.59	89.30
RbTS	960.74	95.26	CsTS	990.48	94.35
RbTS	970.70	96.77	CsTS	1000.39	95.77
RbTS	980.59	95.88	CsTS	1010.32	91.86
RbTS	990.48	102.47	CsTS	1020.25	96.28
RbTS	1000.39	89.95	CsTS	1030.20	92.16
RbTS	1010.32	97.17	CsTS	1040.17	90.67
RbTS	1020.25	92.92	CsTS	1050.15	94.68
RbTS	1030.20	93.84	CsS3	782.00	66.70
RbTS	1040.17	90.63	CsS3	791.47	66.78
RbTS	1050.15	88.65	CsS3	791.94	67.06
RbTS	1060.02	96.01	CsS3	801.41	68.34
RbTS	1069.89	92.65	CsS3	801.84	71.27
CsTS2	791.47	74.18	CsS3	811.34	74.82
CsTS2	791.94	72.17	CsS3	821.22	76.18
CsTS2	801.41	77.36	CsS3	831.18	73.11
CsTS2	801.84	75.98	CsS3	841.14	80.38
CsTS2	811.34	80.18	CsS3	851.15	78.41
CsTS2	821.22	90.89	CsS3	871.07	78.54
CsTS2	831.18	97.99	CsS3	900.91	81.56
CsTS2	841.14	100.86	CsS3	920.73	80.24
CsTS2	851.15	101.14	CsS3	920.79	82.72
CsTS2	861.13	102.20	CsS3	930.69	79.89
CsTS2	881.03	102.34	CsS3	930.79	83.51
CsTS2	890.92	102.85	CsS3	940.61	77.25
CsTS2	900.91	103.03	CsS3	940.79	84.97
CsS3	950.57	78.72	KTS	1397.90	84.84†
CsS3	960.74	80.61	KTS	1502.20	84.75†
CsS3	970.70	78.34	KTS	1609.50	86.34†
CsS3	980.59	82.31	KTS	1694.10	85.02†
CsS3	990.48	84.26	CMTS	1543.30	88.47†
CsS3	1000.39	77.29	CMTS	1590.80	89.79†
CsS3	1010.32	77.82	CMTS	1639.20	85.68†
CsS3	1020.25	77.94	CMTS	1688.10	87.94†
CsS3	1040.17	79.56	CMTS	1734.40	88.90†
CsS3	1060.02	79.78	BTS	1590.80	84.20†
CsS3	1069.89	81.27	BTS	1639.20	89.32†
KTS	1000.20	101.20†	BTS	1688.10	86.96†
KTS	1087.50	100.83†	BTS	1734.40	87.66†
KTS	1190.10	98.85†	BTS	1780.30	83.90†
KTS	1293.70	93.36†			

†data from HT-1500; otherwise data from DSC

must have occurred because the heat capacity (at temperatures below the liquidus) has dropped down to values typical for a crystalline sample. Continued heating of the devitrified sample leads to a sharp increase in C_p reflecting the endothermic effect of melting; the apparent heat capacity reaches much higher values than originally observed for the glass. Clearly, the effect of crystallization and subsequent melting on the C_p vs. T curve is in marked contrast to that observed during the transition from glass to supercooled liquid. This effectively rules out incipient crystallization as an explanation for the anomalous heat capacity behavior of the TiO_2-bearing samples.

Returning to Fig. 1, the most intriguing aspect of the Na_2O-TiO_2-$2SiO_2$ data is that extrapolation of the constant, high temperature liquid C_p value down to the glass transition temperature leads to a change in C_p at T_g of approximately 15.8 J/g.f.w.-K; this is roughly equivalent to the change in C_p at T_g observed for the $Na_2Si_3O_8$ melt (15.0 J/g.f.w.-K). The implication is that the large heat capacity step at T_g in the TiO_2-bearing melt ($\sim$32 J/g.f.w.-K) reflects significant configurational rearrangements in the liquid not available to TiO_2-free silicates. In addition, this "extra" configurational heat capacity apparently decreases and disappears as temperature increases, implying the completion of whatever process is responsible, or the attainment of a random mixture of configurations whose energy differences are negligible relative to the available thermal energy.

This pattern is not restricted to sodic TiO_2-bearing silicate liquids, but is also observed when Ti^{4+} substitutes into K_2O-$3SiO_2$ and K_2O-$2SiO_2$ liquids. For example, Fig. 3 compares calculated C_p values for K_2O-$3SiO_2$ liquid and glass with measured values for liquid and glass K_2O-TiO_2-$2SiO_2$. The calculated C_p values for K_2O-$3SiO_2$ liquid are interpolated from the measured liquid heat capacities for K_2O-$1.3SiO_2$, K_2O-$2SiO_2$, and K_2O-$5SiO_2$ from RICHET and BOTTINGA (1985). The C_p for K_2O-$3SiO_2$ glass was calculated from the model of STEBBINS et al. (1984). Again, the TiO_2-bearing sample displays a jump in C_p at T_g that is exceptionally large, followed by a progressive decrease in liquid C_p for over 400 K, until C_p eventually becomes constant. This negative temperature dependence was also observed by RICHET and BOTTINGA (1985); their fitted C_p curve for this composition is shown in Fig. 3b. Again, extrapolation of the constant C_p at high temperatures down to T_g leads to a jump in C_p of only $\sim$13 J/g.f.w.-K. This is comparable in magnitude to that calculated for K_2O-$3SiO_2$.

A similar pattern is seen for K_2O-$2SiO_2$ and K_2O-TiO_2-SiO_2 liquids. In Fig. 4, the heat capacity measurements of

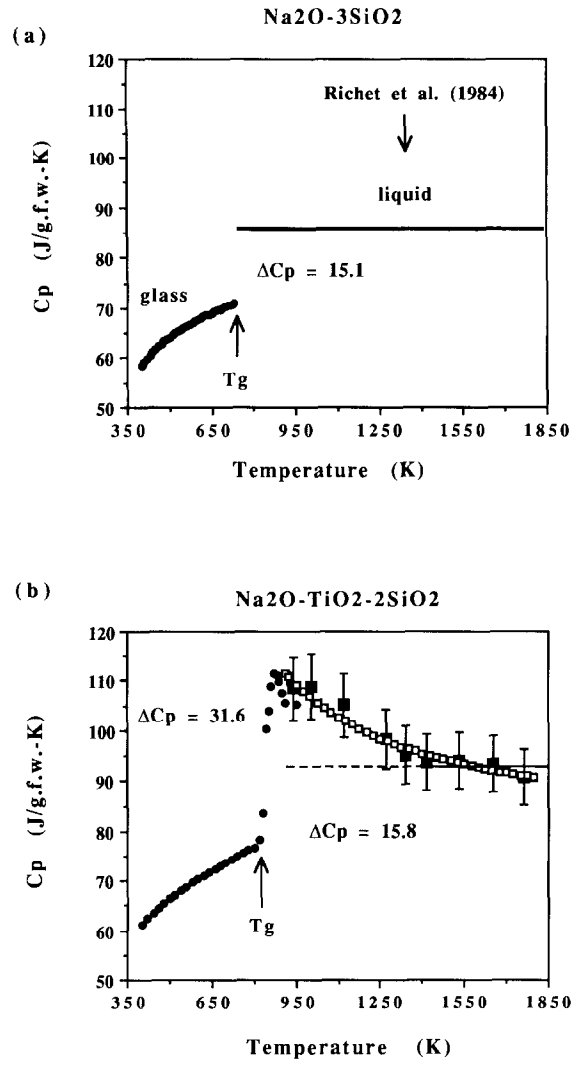

FIG. 1. (a) Heat capacity vs. temperature for Na_2O-$3SiO_2$ liquid and glass from RICHET et al. (1984). ΔCp refers to the jump in heat capacity at the glass transition (T_g). (b) Heat capacity vs. T for Na_2O-TiO_2-$2SiO_2$ glass and liquid from this study. Data obtained using the DSC and the HT-1500 are shown by solid circles and squares, respectively. The open squares represent the fitted curve of RICHET and BOTTINGA (1985) based on their drop calorimetric measurements for this composition.

RICHET and BOTTINGA (1985) for K_2O-$2SiO_2$ are compared to the measurements of this study for K_2O-TiO_2-SiO_2 liquid. Once again, there is a much larger jump in C_p at the glass transition for the Ti^{4+}-bearing sample (although we encountered problems of crystallization immediately above the glass transition). The high temperature C_p data for K_2O-TiO_2-SiO_2 show a strong negative temperature dependence that eventually leads to a constant C_p. Extrapolation of this high temperature value down to T_g leads to a jump in C_p that is somewhat smaller than that observed for the K_2O-$2SiO_2$ sample. Moreover, the liquid C_p data of RICHET and BOTTINGA (1985) for K_2O-$2SiO_2$ liquid show a positive temperature dependence.

DSC measurements of C_p through the glass transition were also made on samples containing Rb_2O and Cs_2O (Fig. 5). For both Rb_2O-TiO_2-$2SiO_2$ and Cs_2O-TiO_2-$2SiO_2$ compositions, a large jump in C_p at T_g is obtained, followed by a decrease in liquid C_p with increasing temperature. To document that the large jump in C_p observed at T_g is not an artifact of the measurements, we also present DSC measurements of C_p through the glass transition for composition Cs_2O-$3SiO_2$. In Fig. 5, it is clear that the jump in C_p at T_g is significantly higher for Cs_2O-TiO_2-$2SiO_2$ than Cs_2O-$3SiO_2$, although the measurements were performed under identical conditions.

High-temperature (1500–1800 K) heat capacity data are also presented for TiO_2-bearing silicate liquids containing the alkaline-earth components BaO, CaO, and MgO (Table 2; Fig. 6). Owing to problems of crystallization, only measurements in the stable liquid region were obtained. In this high-temperature range, no temperature dependence to the liquid heat capacity could be resolved. DSC measurements of C_p were not made on these samples because the glass transition occurs at temperatures that exceed the DSC upper limit (1100 K).

DISCUSSION

Configurational Heat Capacity, Viscosity, and "Fragility"

The data presented in this study demonstrate an unusual behavior of heat capacity with temperature for Ti-bearing alkali silicate liquids and may provide key information on the configurational changes available to them. The configurational changes in silicate liquids with temperature are directly related to their transport and thermodynamic properties and thus are extremely important. For example, the configurational entropy of a silicate liquid directly influences viscosity and diffusivity, as clearly demonstrated by RICHET (1984), RICHET et al. (1986), and NEUVILLE and RICHET (1991) in their application of the ADAM and GIBBS (1965) configurational entropy theory of viscosity to silicate liquids. Richet and others have shown that changes in viscosity with

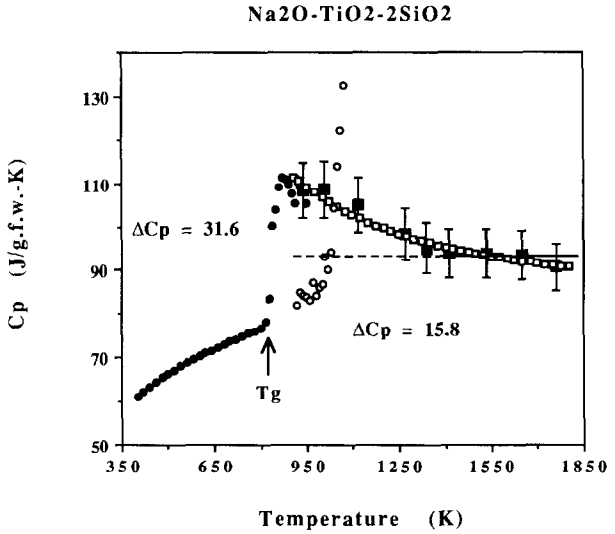

FIG. 2. The same plot as in Fig. 1b, but with additional data (open circles) showing the effect of incipient crystallization following by melting (see text for discussion).

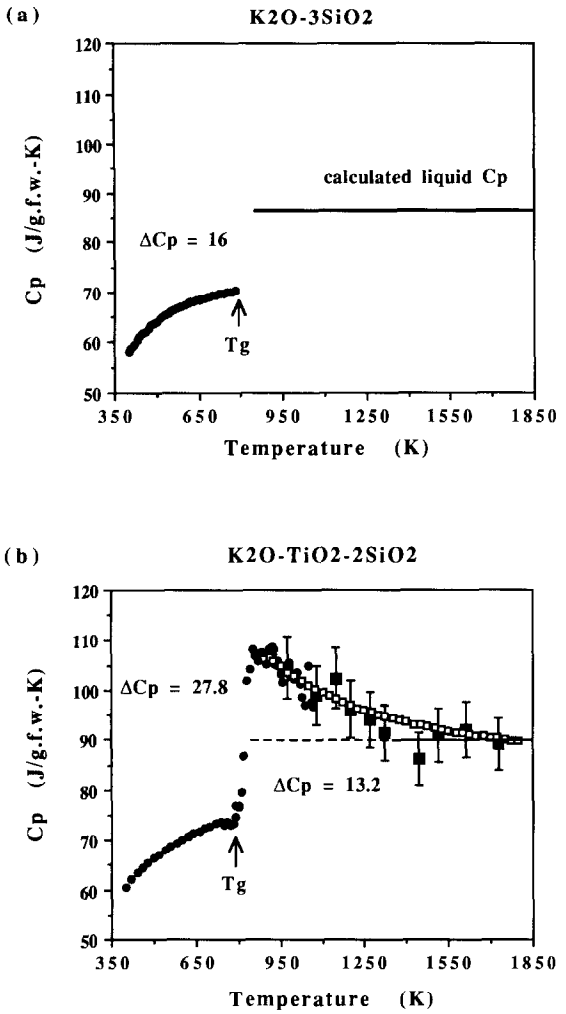

FIG. 3. (a) Heat capacity vs. T for K_2O-$3SiO_2$ liquid and glass (see text for discussion of calculation). (b) Heat capacity vs. temperature on K_2O-TiO_2-$2SiO_2$ glass and liquid. Glass heat capacity is shown by solid circles and was calculated from the model of STEBBINS et al. (1984). Liquid data from the HT-1500 are shown by solid squares. The open squares represent the fitted curve of RICHET and BOTTINGA (1985) based on their drop calorimetric measurements for this composition.

temperature for many silicate and aluminosilicate liquids can be related to configurational entropy (S^{conf}) through the simple relation

$$\log \eta = A + \frac{B}{TS_{conf}(T)}. \quad (1)$$

The change in configurational entropy with temperature is described by the equation

$$S^{conf}(T) = S^{conf}(T_g) + \int (C_p^{conf}(T)/T)dT, \quad (2)$$

where T_g is the glass transition temperature and $C_p^{conf}(T)$ is the configurational heat capacity at temperature T. The magnitude of the configurational heat capacity at T can be determined from the difference between the liquid C_p at T and the glass C_p at T_g. As a glass is heated through its glass transition temperature, an abrupt increase in heat capacity (and other second-order thermodynamic properties) occurs and presumably reflects the sudden achievement of configurational rearrangements in the liquid. STEBBINS et al. (1984) pointed out that constant volume heat capacities (C_v) of silicate liquids can be as much as 1.5 times greater than the ideal harmonic vibrational limit, thus providing strong evidence for a major configurational contribution to liquid heat capacities. A key to understanding the mechanism for viscous flow in silicate melts may lie in identifying what configurational changes take place to provide the additional "heat sink" in liquids relative to glasses.

According to Eqns. 1 and 2, the TiO_2-bearing alkali silicates that exhibit anomalously large changes in C_p at the glass transition (and hence, contain a large configurational contribution to their liquid heat capacity) will also be characterized by a highly non-Arrhenius behavior of viscosity. In a series of papers, ANGELL (1985, 1988) noted that the viscosity-temperature trends of silicate liquids fall between two extremes referred to as "strong" and "fragile." Liquids classified as fragile have structures that change rapidly with increasing

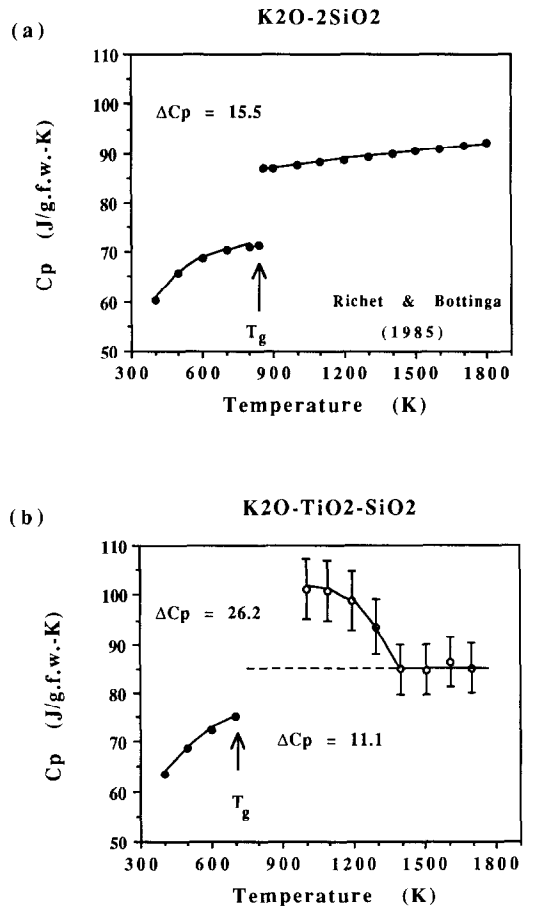

FIG. 4. (a) Heat capacity vs. T for K_2O-$2SiO_2$ liquid and glass from RICHET and BOTTINGA (1985). (b) Heat capacity vs. T for K_2O-TiO_2-SiO_2 glass and liquid. Glass data were calculated from the model of STEBBINS et al. (1984). The solid squares represent liquid data obtained in this study with a Seteram HT-1500 is step-scanning mode.

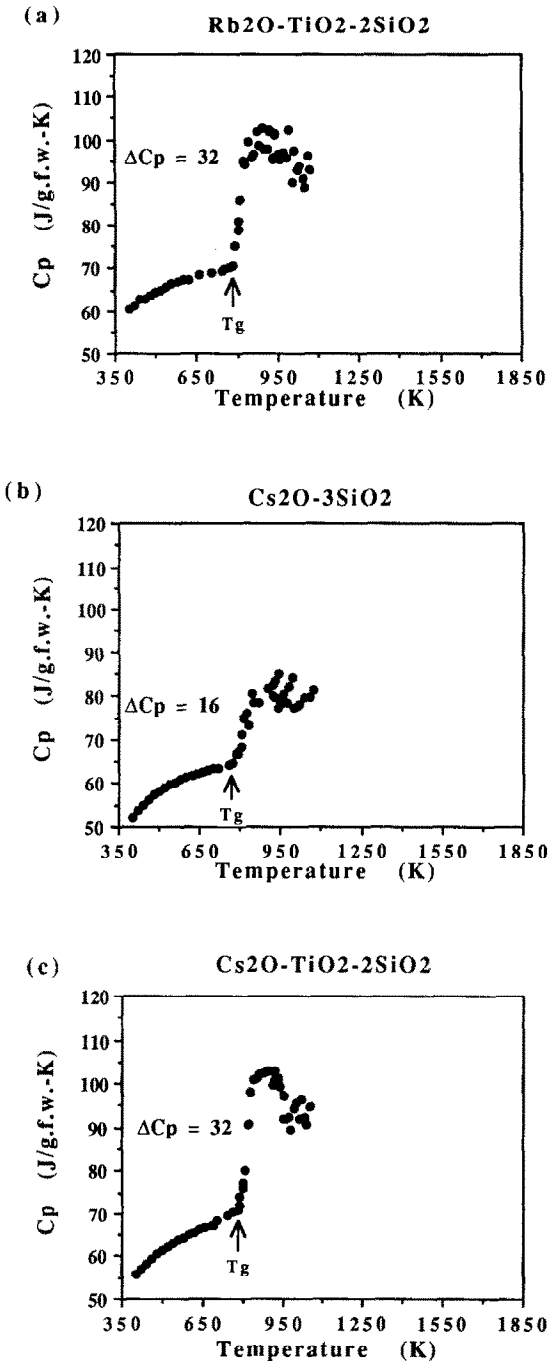

FIG. 5. Heat capacity vs. T for (a) Rb_2O-TiO_2-$2SiO_2$, (b) Cs_2O-$3SiO_2$, and (c) Cs_2O-TiO_2-$2SiO_2$ glass and liquid. Data obtained in this study by differential scanning calorimetry are shown by solid circles.

temperature to those of higher entropy and display non-Arrhenius viscosity-temperature trends. In contrast, strong liquids are those that form fully polymerized tetrahedral networks (such as SiO_2 and GeO_2) and closely follow Arrhenius viscosity behavior. Fragile liquids are further characterized by large changes in C_p at the glass transition, whereas strong liquids display only small changes. SCAMEHORN and ANGELL (1991) stress that although fully polymerized liquids tend to exhibit "strong" behavior, the relationship between fragility and polymerization is not straightforward; there is an additional influence exerted by the Al:Si ratio and the type of countercation (basic oxide) present in the melt.

From the data presented in this study, Ti^{4+}-bearing alkali silicate liquids also fall in the "fragile" class of liquids, owing to the large jump in C_p observed at the glass transition. What structural changes cause this fragile behavior?

The observation that the viscosity of several fully polymerized melts decreases with increasing pressure may also be an important clue to the cause of fragility. The molecular dynamic simulations of SCAMEHORN and ANGELL (1991) indicate that pressure and Al/Si substitution work in similar ways to enhance fragility. Our results indicate that Ti/Si substitution also promotes fragility quite dramatically. The effect of pressure on fully polymerized melts and glasses is to decrease the average T-O-T bond angle and increase T-O bond lengths (SEIFERT et al., 1983; HEMLEY et al., 1986; WILLIAMS and JEANLOZ, 1988). Similarly, a strained T-O-T angle and weakened T-O bonds are also observed in systems of high alumina content (NAVROTSKY et al., 1985) and may be critical for fragile behavior. Substituting Ti^{4+} for Si^{4+} in tetrahedral coordination will lengthen the T-O bond (Ti-O > Si-O) and probably decrease the T-O-T angle (Ti-O-Si < Si-O-

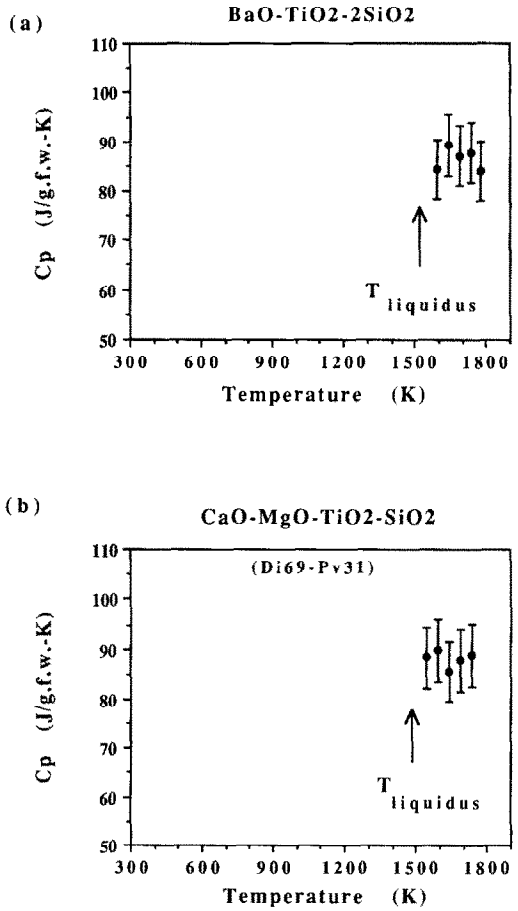

FIG. 6. Heat capacity vs. T for (a) BaO-TiO_2-SiO_2 liquid and (b) CaO-MgO-TiO_2-SiO_2 liquid. Data obtained in this study with a Setaram HT-1500 in step-scanning mode are shown by solid squares.

Si), which should promote fragility. In addition, the results of SCAMEHORN and ANGELL (1991) indicate that an increase in fragility is also linked to increases in the average coordination number of Al^{3+} and Si^{4+}, which is consistent with the lengthening of T-O bonds and the decreasing of T-O-T angles that are observed as coordination numbers increase. Is there evidence for changes in the coordination of Ti^{4+} in alkali silicate liquids, particularly as a function of temperature?

The coordination environment of Si^{4+}, Al^{3+}, and Ti^{4+} in silicate liquids is typically obtained from spectroscopic and EXAFS data on quenched glasses. However, X-ray diffraction studies on both liquids and glasses (TAYLOR and BROWN, 1979; OKUNO and MARUMO, 1982) indicate fundamental differences between the molten and glassy state. Although "strong" liquids such as albite show little change in T-O-T bond angle between glass and liquid (146 vs. 146.4 degrees, respectively), more "fragile" liquids like anorthite display a marked difference (143 vs. 136.4, respectively). There is, in addition, evidence from MAS-NMR experiments that rapidly quenched peraluminous glasses in the CaO-Al_2O_3-SiO_2 system contain 5- and 6-fold coordinated Si^{4+} and Al^{3+}, whereas the same compositions cooled more slowly to a glass contain only 4-coordinated Si^{4+} and Al^{3+} (SATO et al., 1990). A similar pattern was observed by STEBBINS (1991) for $K_2Si_4O_9$ glass quenched at different rates; a higher proportion (0.10 vs. 0.06%) of 5-coordinated Si^{4+} is observed in rapidly quenched glass ($\sim$5–20 $\times$ 10^5 K/min) relative to glass quenched more slowly (1 K/min). Both of these examples illustrate the difficulty of "quenching" the high temperature structure (and higher coordinations of network ions) in silicate liquids.

From the C_p vs. T plots in Figs. 1–4, it is clear that TiO_2-bearing alkali silicate liquids quenched at normal rates will not lead to glasses that represent the liquid structure at high temperatures. The structure frozen into the glass will represent temperatures immediately above the glass transition, and not the stable liquid region. It would be highly useful, therefore, to have an in-situ probe of the coordination of Ti^{4+} in alkali silicate liquids throughout the liquid region. An indirect, but nonetheless in-situ, examination of Ti^{4+} coordination can be obtained from the bulk property, density.

The Partial Molar Volume of TiO_2 in Silicate Melts: Evidence for Different Coordination States

A useful characteristic of many multicomponent silicate liquids is that their volumes can be modelled by the simple equation

$$V_{liq}(T) = \sum X_i V_i(T), \quad (3)$$

where $V_{liq}(T)$ is the measured liquid molar volume, X_i is the mole fraction of oxide component i, and V_i is the fitted partial molar volume of oxide component i. Implicit in this equation is the assumption that the partial molar volumes of the liquid oxide components are independent of composition. LANGE and CARMICHAEL (1987) showed that by considering data obtained only by the double-bob Archedean method (the most precise technique available for measuring the density of molten silicates at one bar), volumes of nonperaluminous K_2O-Na_2O-CaO-MgO-Al_2O_3-SiO_2 liquids could be described as a linear function of composition to a high precision ($\pm$0.2%). However, this assumption of constant partial molar volumes (as a function of composition) breaks down when TiO_2-bearing silicate liquids are considered.

For example, the density measurements of LANGE and CARMICHAEL (1987) and JOHNSON and CARMICHAEL (1987) indicate a strong compositional dependence to the partial molar volume of TiO_2. Specifically, at 1673 K, the fitted value for V_{TiO_2} in silicate liquids containing CaO and MgO is 23.61 $\pm$ 0.35 cc/mol. In contrast, at the same temperature, the fitted values for V_{TiO_2} in sodic and potassic liquids are 29.59 $\pm$ 0.57 and 34.14 $\pm$ 0.90 cc/mol, respectively. These results indicate that the partial molar volume of TiO_2 in silicate liquids increases quite substantially (more than 40%!) as the field strength of the network modifying cation decreases and could reflect a composition-induced change in the coordination of Ti^{4+}. More recent density measurements on TiO_2-bearing liquids by DINGWELL (1992) confirm this trend. Although density measurements are not the most direct probe of melt structure, these results are suggestive regarding Ti^{4+} coordination. Titanium is known to be four-, five-, and sixfold coordinated by oxygen in various crystal structures. A number of recent spectroscopic, X-ray emission, and phase equilibria investigations (YARKER et al., 1986; DICKINSON and HESS, 1985; HANADA and SOGA, 1980; GREEGOR et al., 1983) indicate that similar Ti^{4+} coordinations generally exist in liquids and glasses, though for a given composition, the proportion of different coordinations may depend on temperature.

Another way of looking at the structure of TiO_2-bearing silicate liquids is in terms of alkali-titanate and alkaline earth-titanate complexes as suggested by DICKINSON and HESS (1985). They performed solubility measurements of rutile in two series of liquid compositions within the K_2O-Al_2O_3-SiO_2 and CaO-Al_2O_3-SiO_2 systems, respectively. (Although the liquids in this study are Al-free, it is still useful to consider their results on aluminosilicate liquids.) The much higher solubility of TiO_2 in the potassic melts led DICKINSON and HESS (1985) to suggest the formation of strong complexes between K^+ and Ti and to conclude that Ca^{2+} is not as effective at complexing with Ti. If the "complex" is that of a M^+ (or M^{2+}) cation and a TiO_4 tetrahedron, it is strongest for the most ionic cations as suggested by Raman spectra on quenched alkali titanate glasses (SAKKA et al., 1989). Moreover, the complex apparently breaks down more readily for M^{2+} cations. If the product is mostly octahedral, the "complex" formalism and "coordination number change" formalism may represent descriptions of the same phenomenon.

There is indirect evidence from the volume data that Ti^{4+} is primarily in octahedral coordination in the alkaline-earth silicate melts. Namely, the derived value for V_{TiO_2} at 1673 K of 23.6 cc/mol is similar to the volume of anatase at 1673 K (21.6 cc/mol). When corrections are made for volume of fusion effects (typically 5–10%), the similarity in values suggests that titanium is octahedrally coordinated in these melts as for anatase. In addition, there is no change in V_{TiO_2} between the calcic and magnesian silicate melts, suggesting that if the coordination of Ti^{4+} is predominantly six in the calcic melts, the higher cation field strength of Mg^{2+} relative to Ca^{2+} should

favor this higher coordination as well, and a difference in V_{TiO_2} would not be expected.

In contrast, there appears to be a strong dependence of V_{TiO_2} on the size of the network-modifying cation in the alkali silicate melts, with larger volumes suggestive of lower coordination numbers favored by lower field strengths of monovalent cations. This is consistent with NMR, Raman, and infrared spectroscopy data on silicate glasses quenched from liquids at pressures up to 12 GPa (XUE et al., 1991). Their results indicate that pressure and an increase in the field strength of network modifying cations work in similar ways to enhance Q^n speciation disproportionation (where Q^n refers to the number (n) of bridging oxygens bonded to a tetrahedrally coordinated cation). Q^n speciation disproportionation refers to reactions of the form

$$2Q^n = Q^{n-1} + Q^{n+1}. \quad (4)$$

Reactions driven to the right in Eqn. 4 appear to facilitate the formation of five- and six-coordinated silicon by a mechanism in which nonbridging oxygens are converted to bridging oxygens (cf. XUE et al., 1991: Fig. 13). There is, however, at least one important exception to this general trend. J. F. Stebbins (pers. commun.) has observed that $Na_2Si_4O_9$ glass contains less five-coordinated Si^{4+} than $K_2Si_4O_9$ glass (both glasses quenched at similar rates). This result is opposite to that expected, based on the argument that an increase in disproportionation should favor formation of higher coordinated Si^{4+}.

Currently, we have no idea if the derived value of V_{TiO_2} in the potassic silicate melts represents Ti^{4+} in a predominantly tetrahedral coordination or Ti^{4+} distributed among three coordinations (four, five, and six). We can only surmise that the population of four-fold Ti^{4+} is greater in the potassic vs. sodic melts. Interest in this problem is increased when the anomalous heat capacity data for these TiO_2-bearing alkali silicate melts are also considered.

What Causes the Anomalous Large Jump in C_p at the Glass Transition in the Ti-Bearing Liquids, and Why Does it Decrease and Level Off With Increasing Temperature?

These questions are difficult to resolve definitively with the data currently available. At this point, it is useful to outline what we do and do not know. Firstly, we know there is a large C_p anomaly which indicates significant and reversible restructuring of the melt. Secondly, C_p levels off at high temperature, presumably because whatever change has occurred is either complete or has reached a random mixture of configurations that are effectively of equivalent energy. The list of what we do not know is longer. We cannot distinguish whether the C_p anomaly involves Ti^{4+} coordination change, the breakdown of alkali titanate complexes, or a combination of both. Also, if coordination change does occur, we have no way of evaluating exactly how much four-, five-, and six-coordinated Ti^{4+} is present. Spectroscopic measurements on quenched samples will not provide that information because the configurational changes appear to be reversible and may be quite rapid. In situ density, heat capacity, and viscosity measurements over the temperature range of the anomaly will help. In-situ spectroscopy would provide the best information. Although our understanding is currently limited regarding what is happening at the microscopic level, we can, in the meantime, use the heat capacity data obtained in this study to evaluate the change in the configurational entropy, enthalpy, and free energy of the TiO_2-bearing silicate liquids.

Calculations of Configurational Entropy, Enthalpy, Free Energy, and the Relationship to Viscosity

An important exercise is to calculate the change in the configurational entropy of the TiO_2-bearing and TiO_2-free liquids shown in Figs. 1–3, using the data in Table 2b and the relationship in Eqn. 2. Although the initial configurational entropy at the glass transition is not known, the relative changes in configurational entropy with temperature can be readily computed. Figure 7 presents plots of $S^{conf}(T) - S^{conf}(T_g) = \Delta S^{conf}(T)$ vs. T which show the anomalous changes in configurational entropy with temperature observed

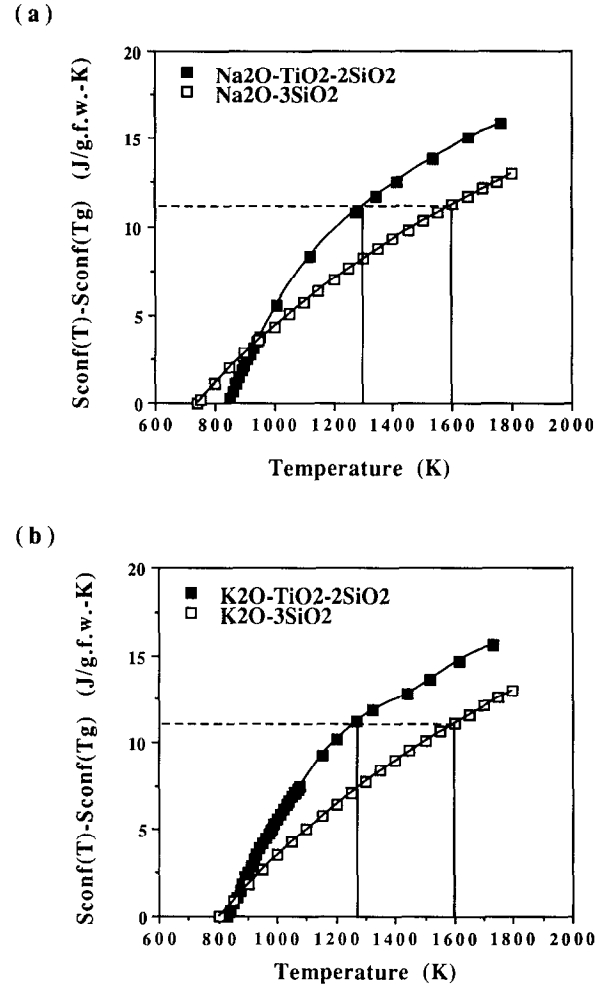

FIG. 7. (a) A plot of the change in configurational entropy with temperature, $S^{conf}(T)$, relative to its value at the glass transition, $S^{conf}(T_g)$, for Na_2O-TiO_2-$2SiO_2$ and Na_2O-$3SiO_2$ liquids. By 1500 K, the difference in the relative configurational entropy between the two liquids is ~3 J/g.f.w.-K. (b) A similar plot for K_2O-TiO_2-$2SiO_2$ and K_2O-$3SiO_2$ liquids. The dashed lines indicates a single value for ΔSconf(T) that corresponds to a difference in temperature of ~300 degrees between the Ti-bearing and Ti-free liquids.

for Na_2O-TiO_2-$2SiO_2$ and K_2O-TiO_2-$2SiO_2$ liquids relative to Na_2O-$3SiO_2$ and K_2O-$3SiO_2$ liquids. Because the TiO_2-bearing samples have higher glass transition temperatures, at temperatures immediately above T_g they have lower configurational entropies relative to the TiO_2-free liquids. However, within a few tens of degrees, the configurational entropies of the TiO_2-bearing liquids rapidly exceed those of the TiO_2-free liquids. This rapid increase in $\Delta S^{conf}(T)$ is directly related to the large jump in C_p at the glass transition observed for the TiO_2-bearing samples. Eventually, at temperatures exceeding 1400 K, the change in ΔS^{conf} with temperature is similar between the TiO_2-bearing and TiO_2-free liquids, reflecting the decrease in liquid heat capacity of the TiO_2-bearing samples to values similar to those of the TiO_2-free melts. At temperatures $\geq$1400 K, however, the $\Delta S^{conf}(T)$ of the TiO_2-bearing liquids are approximately 3.5 J/g.f.w.-K greater than the TiO_2-free liquids at any given temperature. This magnitude difference in ΔS^{conf} is comparable to that caused by raising the liquid temperature by more than 300 degrees.

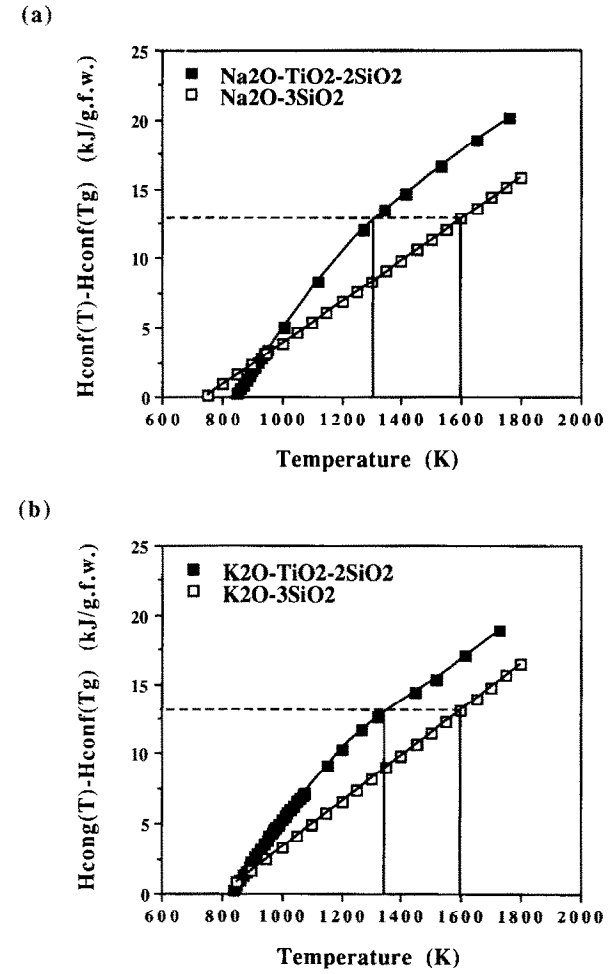

FIG. 8. A similar plot as in Fig. 7 showing the change in configurational enthalpy with temperature relative to that at the glass transition for (a) Na_2O-TiO_2-$2SiO_2$ and Na_2O-$3SiO_2$ liquids and (b) K_2O-TiO_2-$2SiO_2$ and K_2O-$3SiO_2$ liquids. The dashed lines indicate a single value for ΔHconf(T) that corresponds to a difference in temperature of ~250 degrees between the Ti-bearing and Ti-free liquids.

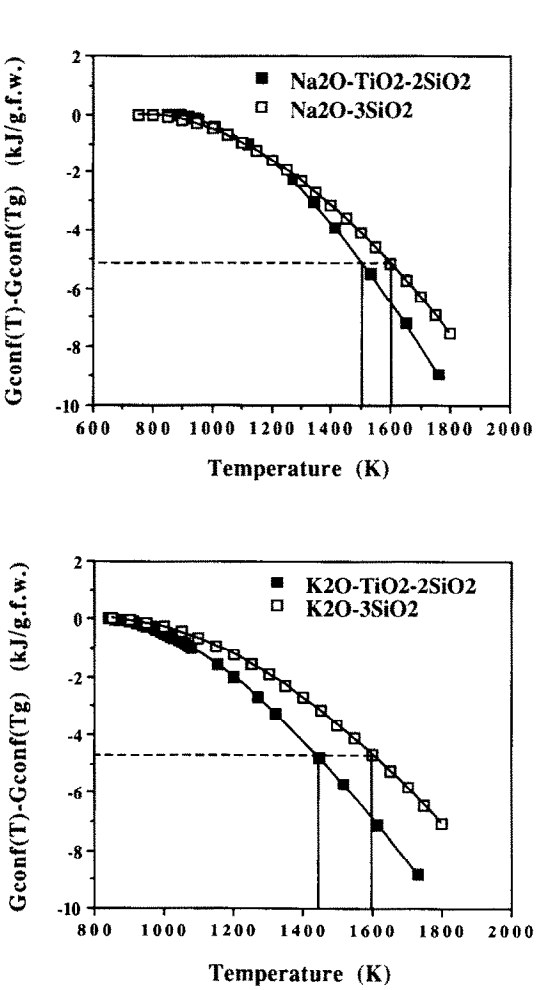

FIG. 9. A similar plot as in Fig. 7 showing the change in configurational free energy with temperature relative to that at the glass transition for (a) Na_2O-TiO_2-$2SiO_2$ and Na_2O-$3SiO_2$ liquids and (b) K_2O-TiO_2-$2SiO_2$ and K_2O-$3SiO_2$ liquids. The dashed lines indicate a single value for $\Delta G^{conf}(T)$ that corresponds to a difference in temperature between the Ti-bearing and Ti-free liquids of ~100 degrees for the sodic melts and ~175 degrees for the potassic melts.

Similar comparisons of the change in the configurational enthalpy and free energy can also be made between the TiO_2-bearing and TiO_2-free alkali silicate liquids (Figs. 8 and 9). The magnitude of $T^*\Delta S^{conf}(T)$ is larger than that of $\Delta H^{conf}(T)$, leading to values of $\Delta G^{conf}(T)$ for the TiO_2-bearing liquids that are more negative than the TiO_2-free liquids above 1400 K. This has to be the case; the restructuring would not occur if it did not lower the free energy. The magnitude difference in $\Delta G^{conf}(T)$ between the TiO_2-bearing and TiO_2-free liquids is approximately 1 and 2 kJ/g.f.w., respectively, for the Na- and K-bearing liquids. These differences in $\Delta G^{conf}(T)$ are comparable to those caused by raising the liquid temperature by 100 and 175 degrees, respectively. It is perhaps significant that the difference in $\Delta G^{conf}(T)$ is greater between the Ti-bearing and Ti-free melts containing K rather than Na. The reason may be related to the fact that the partial molar volume of TiO_2 is larger in potassic vs. sodic melts (~34 vs. 29 cc/mol, respectively). If this

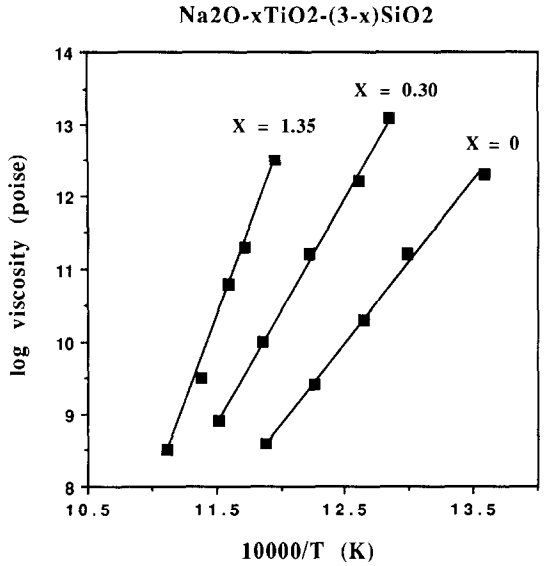

FIG. 10. A plot of log viscosity vs. inverse temperature for three supercooled liquids in the Na_2O-$x TiO_2$-$(3-x)SiO_2$ system. Data shown in solid squares are from HOFFMAN et al. (1952).

represents a larger population of four- and five-coordinated Ti^{4+} in the potassic vs. sodic melts, then this difference in Ti^{4+} coordination may lead to a greater effect on the configurational free energy of the stable liquid. Whether or not this speculation holds, these results clearly demonstrate the energetic magnitude of the configurational changes apparent in the supercooled liquid region and their impact on the thermodynamic properties of the stable liquid (where the anomalous configurational rearrangements appear to have ceased).

The significant differences in $S^{conf}(T)$ between the TiO_2-bearing and TiO_2-free liquids will also be reflected in their viscosity trends with temperature, reflecting the relationship in Eqn. 1. Unfortunately, viscosity measurements on the liquid compositions featured in Figs. 1, 3, and 7 are not available over a wide temperature range. Data are available, however, for Na_2O-$x TiO_2$-$(3-x)SiO_2$ supercooled liquids from HOFFMAN et al. (1952). Their results, shown in Fig. 10, demonstrate that at temperatures immediately above the glass transition, the log η vs. $1/T(K)$ trends are progressively steeper with increasing TiO_2 content of the melts. This is consistent with the lower $S^{conf}(T)$ of the TiO_2-bearing liquids relative to the TiO_2-free liquids at temperatures immediately above the glass transition. However, the data plotted in Fig. 7 indicate that the $S^{conf}(T)$ of the TiO_2-bearing liquids will rapidly exceed that of the TiO_2-free liquids, leading to progressively more shallow log η vs. $1/T(K)$ trends at higher temperatures. The net result will be pronounced curvature in the log η vs. $1/T(K)$ trends of the TiO_2-bearing liquids relative to the TiO_2-free liquids, a common feature of "fragile" liquids. It would be of great interest to verify this prediction with precise viscosity measurements on these liquid compositions over a wide temperature range. Recently, NEUVILLE and RICHET (1991) demonstrated that estimates of the configurational entropy of silicate liquids at T_g can be obtained from viscosity measurements over a wide temperature interval. Such measurements applied to these TiO_2-bearing alkali silicates could provide more quantitative constraints on the anomalous configurational changes that occur, particularly in the supercooled liquid region.

SUMMARY

The most important conclusion drawn from this study is that the presence of TiO_2 has a profound influence on the configurational heat capacity, entropy, enthalpy, and free energy of alkali silicate liquids. Both TiO_2-bearing and TiO_2-free alkali silicates exhibit an abrupt increase in heat capacity at their respective glass transitions, presumably reflecting the sudden achievement of configurational rearrangements in the liquid. What is exceptional about the TiO_2-bearing liquids is that the jump in C_p at T_g is so large, suggesting significant configurational rearrangements in the liquid that may not be available to the TiO_2-free silicates. Moreover, although the "extra" configurational rearrangements in the TiO_2-bearing liquids appear to saturate at high temperatures (in the stable liquid region), they contribute significantly to the configurational entropy and free energy of the stable liquid. This is demonstrated by integration of the function, $C_p^{conf}(T)/T$, to obtain changes in ΔS^{conf} with temperature. Comparison of Na_2O-TiO_2-$2SiO_2$ and K_2O-TiO_2-$2SiO_2$ liquids relative to Na_2O-$2SiO_2$ and K_2O-$3SiO_2$ liquids indicates that the TiO_2-bearing melts have a significantly higher configurational entropy at any given temperature in the stable liquid region. Energetically, this difference in $\Delta S^{conf}(T)$ is equivalent to a difference in temperature of more than 300 degrees. The effect of TiO_2 on the configurational free energy leads to differences that are comparable to changes in temperature of 100 and 175 degrees, respectively, for sodic and potassic liquids. Evaluation of both density measurements on liquids and spectroscopic data on quenched glasses (from the literature) suggests that these energetically important restructuring of the melts may involve temperature-induced changes in Ti^{4+} coordination and/or the breakdown of alkali-titanate complexes. The broad implication for mantle melts is that an increase in the average coordination of Al^{3+} and Si^{4+} will lead to a significant reduction in its free energy; the melt will thus be a stable phase at lower temperatures relative to melts at similar pressures where no coordination change occurred.

Acknowledgments—This work was supported by the National Science Foundation (grant EAR 91-04923 to A. Navrotsky). This paper was improved by comments from J. Stebbins, P. Richet, Y. Bottinga, and P. Hess.

Editorial handling: S. M. McLennan

REFERENCES

ADAM G. and GIBBS J. H. (1965) On the temperature dependence of cooperative relaxation properties in glass-forming liquids. *J. Chem. Phys.* **43**, 139–146.

ANGELL C. A. (1985) Strong and fragile liquids. In *Relaxation in Complex Systems* (ed. K. NGAI and G. B. WRIGHT), pp. 3–11. Natl. Tech. Info. Serv., US Dept. Commerce.

ANGELL C. A. (1988) Perspective on the glass transition. *J. Phys. Chem. Solids* **49**, 863–871.

ANGELL C. A., CHEESEMAN P. A., and TAMADDON S. (1983) Water-like transport property anomalies in liquid silicates investigated at

high T and P by computer simulation techniques. *Bull. Mineral.* **1–2,** 87–99.

CARMICHAEL I. S. E., NICHOLLS J., SPERA F. J., WOOD B. J., and NELSON S. A. (1977) High temperature properties of silicate liquids: applications to the equilibrium and ascent of basic magma. *Phil. Trans. Royal Soc. London* **A286,** 373–431.

DICKINSON J. E. and HESS P. C. (1985) Rutile solubility and titanium coordination in silicate melts. *Geochim. Cosmochim. Acta* **49,** 2289–2296.

DINGWELL D. B. (1992) Density of some titanium-bearing silicate liquids and the compositional dependence of the partial molar volume of TiO_2. *Geochim. Cosmochim. Acta* **56,** 3403–3407.

GREEGOR R. B., LYTLE F. W., SANDSTROM D. R., WONG J., and SCHULTZ P. (1983) Investigations of TiO_2-SiO_2 glasses by X-ray absorption spectroscopy. *J. Non-Cryst. Solids* **55,** 27–43.

HANADA T. and SOGA N. (1980) Coordination of titanium in sodium titanium silicate glasses. *J. Non-Cryst. Solids* **38–39,** 105–110.

HEMLEY R. J., MAO H. K., BELL P. M., and MYSEN B. O. (1986) Raman spectroscopy of SiO_2 glass at high pressure. *Phys. Rev. Lett.* **57,** 747–750.

HOFFMAN L. C., KUPINSKI T. A., THAKUR R. L., and WEYL W. A. (1952) The low-temperature viscosity of glass. *J. Soc. Glass Tech.* **36,** 196–216.

JOHNSON T. and CARMICHAEL I. S. E. (1987) The partial molar volume of TiO_2 in multicomponent silicate melts. *Geol. Soc. Amer. Abstr. Prog. 19,* 719 (abstr.).

KING E. G., ORR R. L., and BONNICKSON K. R. (1954) Low-temperature heat capacity and entropy at 298.16 K and high temperature heat content of sphene ($CaTiSiO_5$). *J. Amer. Chem. Soc.* **70,** 4320–4321.

KUSHIRO I. (1978) Viscosity and structural changes of albite melt at high pressures. *Earth Planet. Sci. Lett.* **41,** 87–90.

LANGE R. A. and CARMICHAEL I. S. E. (1987) Densities of Na_2O-K_2O-CaO-MgO-FeO-Fe_2O_3-TiO_2-SiO_2 liquids: new measurements and derived partial molar properties. *Geochim. Cosmochim. Acta* **51,** 2931–1946.

LANGE R. A. and NAVROTSKY A. (1992) Heat capacities of Fe_2O_3-bearing silicate liquids. *Contrib. Mineral. Petrol.* **110,** 311–320.

LANGE R. A., DEYOREO J. J., and NAVROTSKY A. (1991) Scanning calorimetric measurements of heat capacity during incongruent melting of diopside. *Amer. Mineral.* **76,** 904–912.

NAVROTSKY A., GEISINGER K. L., MCMILLAN P., and GIBBS G. V. (1985) The tetrahedral framework glasses and melts-inferences from molecular orbital calculations and implications for structure, thermodynamics, and physical properties. *Phys. Chem. Minerals* **11,** 284–298.

NEUVILLE D. R. and RICHET P. (1991) Viscosity and mixing in molten (Ca, Mg) pyroxenes and garnets. *Geochim. Cosmochim. Acta* **55,** 1011–1019.

OKUNO M. and MARUMO F. (1982) The structures of anorthite and albite melts. *Mineral. J.* **11,** 180–196.

RICHET P. (1984) Viscosity and configurational entropy of silicate melts. *Geochim. Cosmochim. Acta* **48,** 471–483.

RICHET P. and BOTTINGA Y. (1985) Heat capacity of aluminum-free liquid silicates. *Geochim. Cosmochim. Acta* **49,** 471–486.

RICHET P., BOTTINGA Y., and TEQUI C. (1984) Heat capacity of sodium silicate liquids. *J. Amer. Ceram. Soc.* **67,** C6–C8.

RICHET P., ROBIE R. A., and HEMINGWAY B. S. (1986) Low-temperature heat capacity of diopside glass (CaMgSi2O6): a calorimetric test of the configurational entropy theory applied to the viscosity of liquid silicates. *Geochim. Cosmochim. Acta* **50,** 1521–1533.

RICHET P., ROBIE R. A., ROGEZ J., HEMINGWAY B. S., COURTAIL P., and TEQUI C. (1990) Thermodynamics of open networks: ordering and entropy in $NaAlSiO_4$ glass, liquid, and polymorphs. *Phys. Chem. Minerals* **17,** 385–394.

ROBIE R. A., HEMINGWAY B. S., and FISHER J. R. (1978) Thermodynamic properties of minerals and related substances at 298.15 K and 1 bar (105 Pascals) pressure and at higher temperature. *US G.S. Bull. 1452.*

SAKKA S., MIYAJI F., and FUKUMI K. (1989) Structure of binary K_2O-TiO_2 and Cs_2O-TiO_2 glasses. *J. Non-Cryst. Solids* **112,** 64–68.

SATO R., MCMILLAN P., DUPREE R., and DENNISON P. (1990) MAS-NMR investigation of Al and Si coordination in aluminosilicate glasses. *V. M. Goldschmidt Conf. Abstr.,* **79.**

SCAMEHORN C. A. and ANGELL C. A. (1991) Viscosity-temperature relations in fully polymerized aluminosilicate melts from ion dynamics simulations. *Geochim. Cosmochim. Acta* **55,** 721–730.

SCARFE C. M., MYSEN B. O., and VIRGO D. (1987) Pressure dependence of the viscosity of silicate melts. In *Magmatic Processes: Physiochemical Principles; Special Publication 1,* pp. 59–67. The Geochem. Soc.

SEIFERT F. A., MYSEN B. O., and VIRGO D. (1983) Raman study of vitreous silica. *Phys. Chem. Glasses* **24,** 141–145.

STEBBINS J. F. (1991) NMR evidence for five-coordinated silicon in a silicate glass at atmospheric pressure. *Nature* **351,** 638–639.

STEBBINS J. F., CARMICHAEL I. S. E., and MORET, L. K. (1984) Heat capacities and entropies of silicate liquids and glasses. *Contrib. Mineral. Petrol.* **86,** 131–148.

TAYLOR M. and BROWN G. E. (1979) Structure of mineral glasses - I. The feldspar glasses $NaAlSi_3O_8$, $KAlSi_3O_8$, $CaAl_2Si_2O_8$. *Geochim. Cosmochim. Acta* **43,** 61–75.

WATERS F. C. (1987) A suggested origin of MARID xenoliths in kimberlites by high pressure crystallization of an ultrapotassic rock such as lamproite. *Contrib. Mineral. Petrol.* **95,** 523–533.

WILLIAMS Q. and JEANLOZ R. (1988) Spectroscopic evidence for pressure-induced coordination changes in silicate glasses and melts. *Science* **235,** 902–905.

XUE X., STEBBINS J., KANZAKI M., MCMILLAN P. F., and POE B. (1991) Pressure-induced silicon coordination and tetrahedral structural changes in alkali oxide-silica melts up to 12 Pa: NMR, Raman, and infrared spectroscopy. *Amer. Mineral.* **76,** 8–26.

YARKER C. A., JOHNSON P. A. V., WRIGHT A. C., WONG J., GREEGOR R. B., LYTLE F. W., and SINCLAIR R. N. (1986) Neutron diffraction and EXAFS evidence for TiO_5 units in vitreous K_2O-TiO_2-$2SiO_2$. *J. Non-Cryst. Solids* **79,** 117–136.